GEOPHYSICS, VOL. 71, NO. 6 (NOVEMBER-DECEMBER 2006); P. G279–G284, 5 FIGS.
10.1190/1.2349222

Some characteristics of the electromagnetic field from radio transmitters in Europe

Laust B. Pedersen[1], Mehrdad Bastani[2], and Lars Dynesius[1]

ABSTRACT

The radiomagnetotelluric (RMT) method utilizes man-made signals generated by distant transmitters or by dedicated local transmitters. Man-made electromagnetic (EM) signals in the 1–250-kHz frequency band come mainly from two sources: (1) distant radio transmitters operating in the 15–250-kHz band and (2) nearby or distant industrial sources emitting either transients or higher harmonics of 50 Hz. The natural or background EM signals form a kind of noise floor. In Europe for the 15–250-kHz band, there generally are sufficient transmitters available to estimate the EM transfer functions completely, i.e., the full impedance tensor and the tipper vector. We show examples of the variability of power spectra and azimuthal distributions of transmitters from sites in Sweden, Hungary, The Netherlands, and Spain. We also show that the estimated transfer functions are stable as a function of time; even under typical noisy conditions, simple stacking of spectra in narrow frequency bands provides good-quality estimates of transfer functions.

INTRODUCTION

Plane-wave, natural-source electromagnetic (EM) methods — magnetotellurics (MT) and geomagnetic depth soundings (GDS) — traditionally are used to study the electrical properties of the deep crust and upper and lower mantles. These methods are relatively cheap, and the source is always available, although its strength varies throughout the day and the year. Through the distribution of source currents in the ionosphere and lightning currents in the atmosphere, the corresponding induced current systems in the earth generally flow in all horizontal directions if integrated over a sufficiently long time. This means that measurements of the three components of the magnetic field and the two horizontal components of the electric field at any given position and frequency can be used to set up unique linear relations between the horizontal magnetic field on the one side (input) and the other components on the other side (output).

The so-defined impedance tensor $\mathbf{Z}$ and tipper vector (A,B) are independent of source parameters and only contain information about the electrical conductivity distribution of the earth [Cantwell (1960); see Pedersen and Oskooi (2004) for a review]. Because of the plane-wave nature of the source field, it is much less complicated and faster to model the variation of $\mathbf{Z}$ and (A,B) as a function of frequency and space coordinates compared with the case when the geometry of the source must be taken into account.

The forward and inverse plane-wave modeling techniques developed for deep-earth studies can be applied directly in shallow exploration using the radiomagnetotelluric (RMT) method. A wealth of 1D (Fischer et al., 1981; Parker and Whaler, 1981; Constable et al., 1987; Pedersen and Rasmussen, 1989; Parker and Booker, 1996) and 2D (de Groot-Hedlin and Constable, 1990; Wu et al., 1993; Siripunvaraporn and Egbert, 2000) models exists for that purpose. Recently, full 3D models have been used for inverse modeling (Newman et al., 2003; Siripunvaraporn et al., 2004; Siripunvaraporn et al., 2005). At the present stage of development, routine inversion of MT data using 1D and 2D models can be done using standard personal computers, but 3D inversion still requires that special computers be used because of excessive processing times.

Prospecting for natural resources and environmental effects in the upper few hundred meters of the earth's crust using natural plane-wave sources is difficult because of weak source fields and strong noise in the 1–500-kHz frequency band. In this frequency range, it is better to use controlled sources situated sufficiently far away that their EM fields can be considered a plane. Goldstein and Strangway (1975) show that for a homogeneous half-space, plane-wave conditions prevail if the distance between source and receiver is at least three to five skin depths. For more complicated structures involving highly resistive units, such as crystalline basement, the situation is more complicated. Wannamaker (1997) notes that conductive sediments over resistive basement can reduce the depth of exploration

Manuscript received by the Editor May 23, 2005; revised manuscript received March 21, 2006; published online October 2, 2006.
[1]Uppsala University, Department of Earth Sciences, Villavägen 16, 752 36 Uppsala, Sweden. E-mail: laust.pedersen@geo.uu.se; lars.dynesius@geo.uu.se.
[2]Formerly Uppsala University, Department of Earth Sciences; presently, Geological Survey of Sweden, Villavägen 18, 752 36 Uppsala, Sweden. E-mail: mehrdad.bastani@sgu.se.

significantly within the plane-wave regime (the far-field) to about 5% of the transmitter-receiver distance.

Traditionally, grounded dipole sources have been used in these studies because of their greater range (typically up to 10 km for a 500-m dipole length and a 10-A current). In shallow experiments, it is more advantageous to use horizontal magnetic dipoles because they are much easier to install and their range extends to approximately 1 km (Pedersen et al., 2005). Magnetic dipoles also couple less to nearby conductive structures than electric dipoles and therefore are generally expected to provide better plane-wave conditions than electric dipoles (Qian and Pedersen, 1992).

In the scalar RMT technique, only one horizontal electric and the perpendicular horizontal magnetic component are measured using analog electronics (Turberg et al., 1994; Stiefelhagen and Müller, 1997; Bosch et al., 1999; Tezkan, 1999; Tezkan et al., 2000) for a few transmitters favorably located with respect to the measured electric-field component. In the tensor RMT technique (Pedersen et al., 2005), all five EM components are measured simultaneously using digital technology. Thus, it becomes possible to take advantage of all transmitters that can be received at a particular site at a given time, avoiding the problems that arise because of transmitter instability. Provided the number of available transmitters is sufficient and that their azimuths as seen from the measuring area have a reasonable scatter, it becomes possible to estimate the complete impedance tensor and tipper vector in the 15–250-kHz frequency band (Bastani and Pedersen, 2001).

The advantage of tensor measurements over scalar measurements is particularly pronounced in complex geology where deviations from 1D or 2D geometry can distort the interpretation of the data severely if not taken into account properly. Another advantage is the ability to make inferences about azimuthal anisotropy directly from the measurements (Linde and Pedersen, 2004) without the need to rotate the measurement setup in several steps, as is required for dc geoelectric measurements (Habberjam, 1972; Ritzi and Andolsek, 1992; Matias, 2002; Boadu et al., 2005).

This article shows that the distribution of transmitters, with regard to their frequency and their azimuths as seen from selected sites in Europe, is favorable for tensor RMT measurements. We also show that the stability of the estimated transfer functions is excellent even in an environment of high EM noise.

EM WAVES FROM SOURCE TO RECEIVER

Man-made EM signals used in the RMT method vary as a function of distance and azimuth from transmitters as well as of time. In the following section, we describe some of their characteristics.

Propagation of radio waves in the earth-ionosphere wave guide

The EM signals emitted from powerful transmitters coupled to the ground either as vertical or horizontal electric dipoles travel in the wave guide formed by the earth's surface and the ionosphere. Because of variations in the ionosphere's height and its electrical properties, the field at a given site varies as a function of time — sometimes by more than 50% during solar flare events (Vallée et al., 1992b) over several dozen minutes. The field also varies in a complicated way as a function of distance away from the transmitter as a result of interference between the various modes, e.g., the ground wave and the first sky hop (Vallée et al., 1992a).

The variation of field strength in itself is not a problem for RMT measurements because transfer functions relating the EM components at a given frequency are sought rather than the absolute level of the fields themselves. However, if these variations are accompanied by changes in the modal patterns, leading to large variations in the surface impedances as measured by Thiel and Chant (1982), then care must be exercised in using these techniques a few hours after sunrise and sunset. Later, we study whether this phenomenon affects the estimation of transfer functions over the entire frequency band.

RMT transmitters

In most populated areas of the world, a large number of radio transmitters, including very-low-frequency (VLF) transmitters, can be utilized for geophysical purposes. For example, in Sweden and The Netherlands, 36 remote transmitters in 1998 could be received, covering the 14–250-kHz band. These transmitters provide excellent far-field S/N ratio conditions and thus provide potential sources for estimating plane-wave transfer functions: the impedance tensor and the tipper vector. These sources traditionally have been used in VLF (e.g., McNeill and Labson, 1989; McNeill, 1991; Guerin and Benderitter, 1995) and RMT (e.g., Turberg et al., 1994; Tezkan et al., 1996) techniques as fast, simple ways to derive scalar estimates of earth response functions.

In certain parts of the world, the use of VLF and radio signals is limited to a rather small number of very powerful remote transmitters. This is one reason why a simple local magnetic (or electric) dipole transmitter can be helpful. Another reason is that below about 15 kHz, there are no transmitters, except net harmonics, which may or may not be considered to be in the far-field. Thus, for practical reasons and to ensure good data quality and adequate coverage of signals, the 1–15-kHz band must be covered using a local transmitter. We use a simple automatic transmitter with two perpendicular horizontal magnetic dipoles. We transmit one frequency and polarization at a time and achieve excellent data quality up to about 500 m (Pedersen et al., 2005).

Although the natural EM field has a very broad spectrum with considerable energy (Smith and Jenkins, 1998) in parts of the RMT band, defined here as starting from about 1 kHz and ending at 250 kHz, no serious attempts have been made to use it for exploration purposes. This is in contrast to the situation for the band between 1 Hz and 1 kHz, which is used routinely in AMT surveys throughout the world (Takasugi et al., 1992; Zhang et al., 1995; Brasse and Rath, 1997; Courteaud et al., 1997; Meju et al., 1999). The strength of the natural EM signal in the 1–15-kHz band is very low, and only with special efforts and long integration times can useful results be obtained (Garcia and Jones, 2002).

The EM spectrum was, by custom and practice, divided into 26 alphabetically designated bands. This usage still prevails to some degree. The lowest bands of interest in this context are extra-low frequency (ELF, 30–300 Hz), voice frequency (VF, 300 Hz–3 kHz), very low frequency (VLF, 3–30 kHz), low frequency (LF, 30–300 kHz), and medium frequency (MF, 300–3000 kHz).

One example of measured spectra covering the 10–500-kHz band is given in Figure 1. The traditional VLF transmitters can be identified clearly in the 14–20-kHz band. A gap exists to the next band at 44–80 kHz, lying in the lower part of the LF band. Another gap exists between this band and the upper part of the LF radio 100–250-kHz band. An example of the azimuthal distribution of transmitters

from a site in Sweden can be studied from Figure 2. Note that directions are more or less uniformly distributed, allowing for stable transfer function estimates.

S/N RATIOS IN EUROPE

The S/N ratio is a function of transmitter strength and distance to the transmitter as well as the level and character of local noise. The signal is approximately monochromatic, and the noise depends on the bandwidth used, which in this case is 122 Hz, corresponding to a sampling frequency of 2 MHz and 16,000 samples per stack. The S/N ratio (in decibels) is defined as 10 times the logarithm of the ratio between the power and the background power at a particular frequency. The latter is estimated by applying a median filter to the power spectrum, stacked enough times to obtain stable estimates (Bastani, 2001). We typically use 10 stacks (Pedersen et al., 1994). If the S/N ratio is larger than a preset threshold (typically 12 dB), then a transmitter is picked.

Note that S/N ratios can be increased by decreasing the distance between digital frequencies. This can be done by increasing the total sampling time per data segment or by making use of the fact that most transmitters have a sufficiently high phase stability to allow for stacking of complex amplitudes rather than stacking auto- and cross-powers, as we do here. With Gaussian noise, the S/N ratio increases roughly linearly with the total sampling time per data segment if the signal can be considered to be monochromatic in the measuring time interval.

Because the magnetic and horizontal electric components are measured simultaneously, S/N ratios can be formed for the powers of the horizontal magnetic and electric fields separately. We show both ratios except for the Collendoorn site (The Netherlands) where only magnetic S/N ratios were calculated. Figure 3a shows the results from the Collendoorn area. Most S/N ratios lie above 20 dB, but a few isolated transmitters or transmitters represented by a few neighboring frequencies show smaller values.

Figure 3b shows the results from Skediga, situated approximately 5 km north of Uppsala, Sweden. Notice that the S/N ratio for the electric field is generally much smaller than the one for the magnetic field because the electric field contains a lot of spikelike noise generated by local power consumers placed a considerable distance away from the measurement area. The crystalline bedrock is very resistive (about 10,000 ohm-m), whereby the propagation of electric disturbances over distances of several skin-depth units is facilitated without giving rise to comparable noise in the magnetic fields. At frequencies above 160 kHz, the two S/N levels are very similar, perhaps reflecting that the spike generators now lie in the far-field.

Figure 3c shows the results from Almuñecar, Spain. The field area, a plantation of custard apple trees, is situated a few hundred meters from the town, and much EM noise is generated by power lines and a number of electric pumps used to pump water into irrigation channels feeding the trees. As in the Swedish case, the electric S/N ratio generally lies below the magnetic one except for the higher frequencies, where they are very similar in magnitude. Note that the 80–150-kHz band is void of transmitters. This gap is much wider than in the cases of Sweden and The Netherlands.

Figure 3d shows the results from measurements in Budapest City, Hungary, in the garden of the Budapest Convention Center. From 80–128 kHz, there are no transmitters. However, the S/N ratios of the transmitters found are very similar to those in Spain.

The signal strengths of all transmitters at the four areas are shown in Figure 4. Generally speaking, the variation in power for a particular transmitter is on the order of one decade, probably reflecting the variation in distance between the transmitters and the receiver for each site. One exception is the Collendoorn site, which for some frequencies exhibits much larger signal power than the three other areas. The reason is that many transmitters are located close to Collendoorn, including transmitters in southern England, The Netherlands, Belgium, and western Germany.

The length of the median filter has some influence on the estimated background level, depending on the statistical nature of the power spectrum. We have used a smaller length for the median filter at Collendoorn than for the three other cases. This partly explains why the Collendoorn S/N ratios lie in the same range as for the three other cases, even though the signal level at Collendoorn is significantly higher.

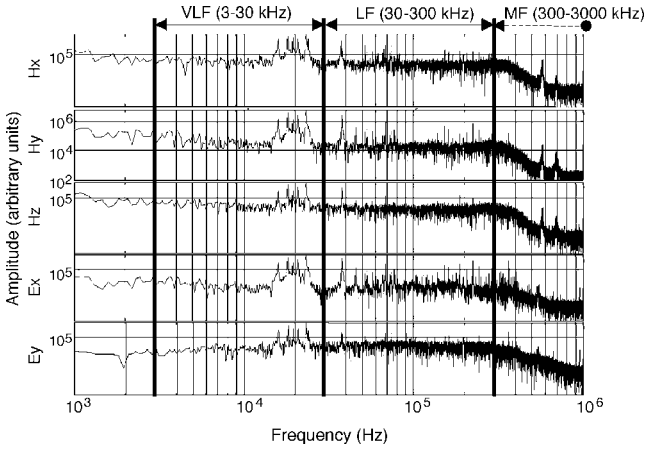

Figure 1. Electromagnetic spectra in Collendoorn, The Netherlands, November 1998, 10–500-kHz band. The symbols H_x, H_y, H_z, E_x, and E_y denote the three magnetic and the two horizontal electric components, respectively. Units on the vertical axes are arbitrary. The decay observed around 500 kHz is the result of an analog low-pass filter.

REPRODUCIBILITY OF EARTH RESPONSES

There has been some debate about the stability of VLF response functions with regard to changing source-field conditions. For example, Thiel and Chant (1982) report on measurements on wave tilt — the ratio between the horizontal electric and magnetic fields — from a transmitter in western Australia situated 4000 km away from

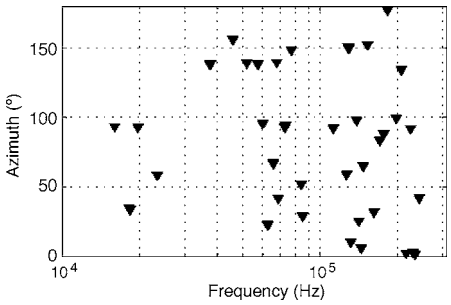

Figure 2. Azimuthal distribution of RMT transmitters, Rockney, Sweden, in the 10–250-kHz band. Direction is found from the minor axis of the polarization ellipse of the horizontal magnetic field.

a receiver in eastern Australia. Using a buried, ungrounded electric-field setup and a shielded loop antenna for the magnetic field, they found a dramatic reduction of wave tilt (proportional to the square root of the apparent resistivity) during a period of a few hours after sunset and sunrise. However, the phase difference between the two fields did not show a similar variation, although standard errors of the phase were as high as 5°. Thiel and Chant (1982) suggest that an explanation can be the complex interference between different wave guide modes that dominate during night and daytime conditions.

To test this effect and to study the stability of the transfer functions over time, we set up an experiment outside the lab at Uppsala. We took a measurement every minute starting at sunset on November 26 and continued for 140 minutes. We calculated the impedance and tipper vector as a function of frequency over the range of 10–250 kHz, involving approximately 40 transmitters. To estimate the transfer functions, we used the parametric approach of Bastani and Pedersen (2001), where each transfer function is represented as a sum of simple functions whose amplitudes are determined using a truncated singular-value decomposition (SVD) approach to estimate the impedance tensor describing the linear filter between the horizontal magnetic field as input and the horizontal electric field as output. Apparent resistivities and phases and their standard errors were then calculated from the off-diagonal elements of the impedance tensor for a set of frequencies half an octave apart.

The results for apparent resistivity corresponding to north-south current flow are shown in Figure 5. Note that apparent resistivities appear to be stable within their measurement error, typically 4% for apparent resistivity. The corresponding phases (not shown here) have typical errors of 1°. Note also that the simple stacking procedure sometimes fails to suppress the scatter to that level.

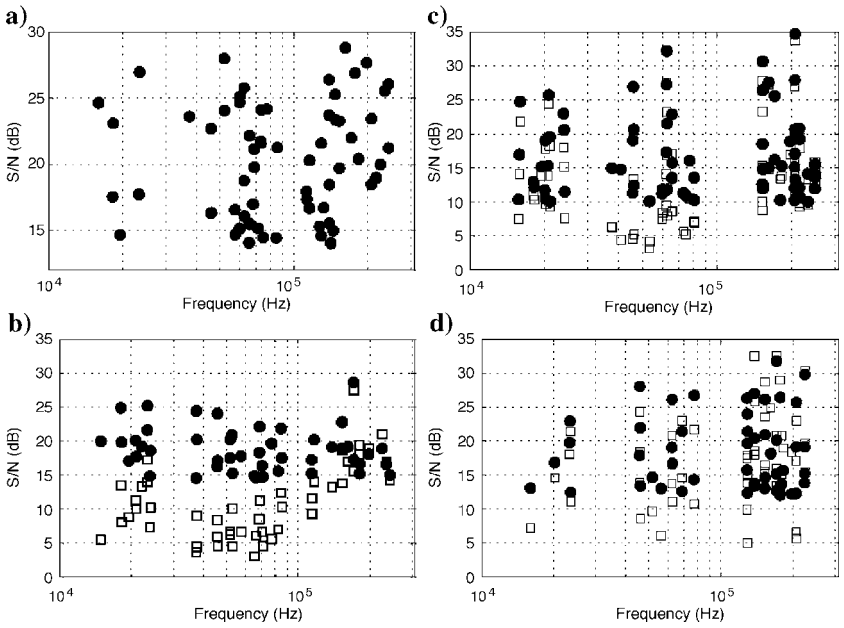

Figure 3. S/N ratios for four different sites. Filled circles denote horizontal magnetic field. Open squares denote horizontal electric field. (a) Collendoorn, The Netherlands, November 1998. (b) Skediga, Uppsala, Sweden, November 1999. (c) Almuñecar, Spain, April 1999. (d) Budapest Convention Center, Hungary, September 1999.

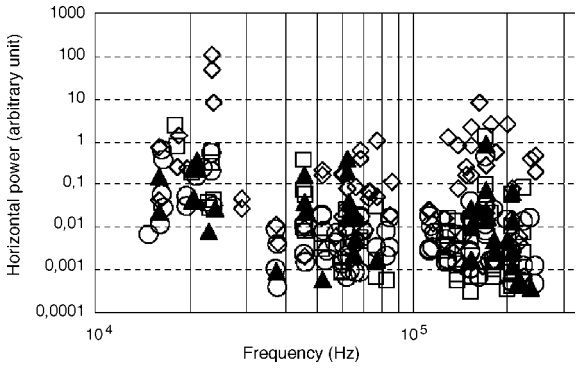

Figure 4. Power of horizontal magnetic field for picked transmitters. Open diamonds: Collendoorn, The Netherlands. Open squares: Budapest, Hungary. Filled triangles: Almuñecar, Spain. Open circles: Uppsala, Sweden.

DISCUSSION

In the real case, the distribution of transmitters is not ideal, as we have demonstrated for several locations in Europe; there are frequency bands in which no transmitters can be found and the azimuthal distribution of transmitters in other bands is nonuniform. To overcome the lack of transmitters and their nonuniform azimuthal distribution, we use a parametric representation of the earth response functions whose coefficients are estimated by an SVD approach, where all signals identified as transmitter signals are used for the estimation process.

In industrial areas, we often find a higher S/N ratio for the magnetic field than for the electric field. This can be interpreted as near-field effects from man-made noise sources that are galvanically coupled to the ground, whereby the electric field dominates the magnetic field as compared to far-field conditions (Li and Pedersen, 1992). To reduce bias effects (Pedersen, 1982), we consider the horizontal magnetic field as input and the horizontal electric field as output to the linear filter defining the impedance tensor.

We see no sign of the variation in the impedance tensor observed by Thiel and Chant (1982) up to two hours after sunset and sunrise. On the contrary, the scatter in the estimates of the off-diagonal elements of the impedance tensor is generally below 1%. We do not understand why Thiel and Chant see such variations; it may be because they measured the electric field by nongrounded dipoles, whereas we use grounded dipoles. In the case of a grounded dipole, we measure the potential difference in the ground between two points, which is directly proportional to the horizontal electric field in the direction of the dipole but independent on the dominant vertical electric field right above the ground from the vertical transmitter dipoles used in standard radio communication.

The ratio between the horizontal and the vertical electric fields is given approximately as the square root of the ratio between the displacement current in the air and the conduction current in the ground (McNeill and Labson, 1989). The horizontal electric field is typically 1%–10% of the vertical electric field. In the case of an ungrounded dipole, there could be a stronger coupling to the vertical electric field in the air, perhaps from a slight misalignment of the dipoles or asym-

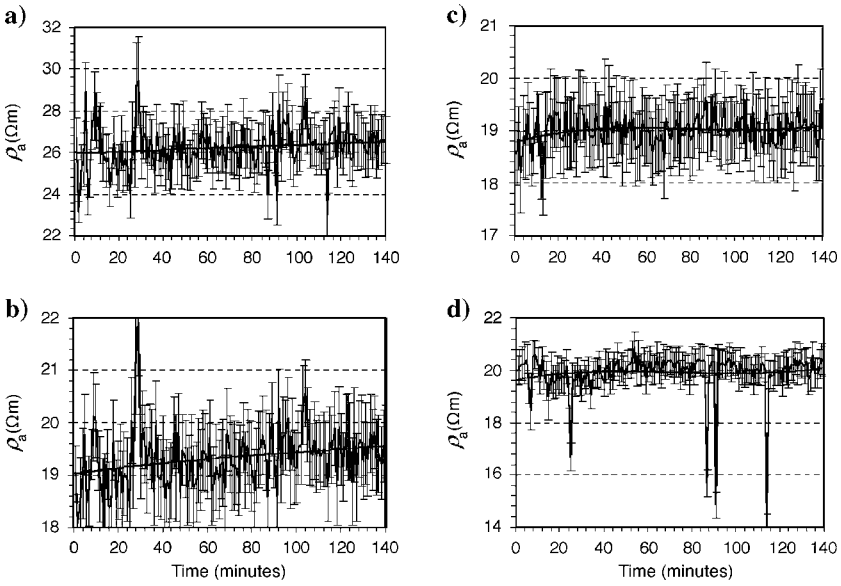

Figure 5. Time stability of transfer functions with error bars. Apparent resistivities (ohm-m) corresponding to current flow from north to south as a function of time (minutes) for (a) 20, (b) 40, (c) 80, and (d) 160 kHz.

metries in their radiation patterns so that they become sensitive to the vertical electric field. Future experiments with ungrounded electric dipole sensors might resolve the problem.

CONCLUSION

The distribution of radio transmitters in Europe is dense enough that their plane-wave EM fields can be used to estimate EM transfer functions in the 15–250-kHz band. It appears that the largest number of transmitters can be received close to the sea, supposedly because of their use for navigational purposes in the coastal areas. We can obtain an estimate of the minimum number of transmitters by assuming that transfer functions are constant in half-octave bands. If the 15–250-kHz band covers about seven half-octave bands and if we need two independent transmitters in each band to define the impedance tensor and tipper vector uniquely, then at least 14 transmitters are required for an ideal distribution of transmitters. In The Netherlands and Hungary, we could receive about 40 and 25 stations, respectively.

REFERENCES

Bastani, M., 2001, EnviroMT — A new controlled source/radiomagnetotelluric system: Uppsala Dissertations from the Faculty of Science and Technology, **32**, Em4.

Bastani, M., and L. B. Pedersen, 2001, Estimation of MT transfer functions from radio transmitters: Geophysics, **66**, 1038–1051.

Boadu, F. K., J. Gyamfi, and E. Owusu, 2005, Determining subsurface fracture characteristics from azimuthal resistivity surveys: A case study at Nsawam, Ghana: Geophysics, **70**, B35–B42.

Bosch, F. P., S. Szalai, P. Turberg, and I. Müller, 1999, Continuously recording radio-frequency EM (RM-EM) method (15–300 kHz) without ground contact: A powerful tool for groundwater vulnerability mapping in fissured rocks: Proceedings from the 5th meeting of the Environmental and Engineering Geophysical Society, European Section.

Brasse, H., and V. Rath, 1997, Audiomagnetotelluric investigations of shallow sedimentary basins in northern Sudan: Geophysical Journal International, **128**, 301–314.

Cantwell, T., 1960, The detection and analysis of low frequency magnetotelluric signals: Ph.D. thesis, Massachusetts Institute of Technology.

Constable, S. C., R. L. Parker, and C. G. Constable, 1987, Occam's inversion: A practical algorithm for generating smooth models from electromagnetic data: Geophysics, **52**, 289–300.

Courteaud, M., M. Ritz, B. Robineau, J. L. Join, and J. Coudray, 1997, New geological and hydrogeological implications of the resistivity distribution inferred from audiomagnetotellurics over La Fournaise young shield volcano (Reunion Island): Journal of Hydrology, **203**, 93–100.

de Groot-Hedlin, C., and C. S. Constable, 1990, Occam inversion to generate smooth, two-dimensional models from magnetotelluric data: Geophysics, **55**, 1613–1624.

Fischer, G., P. A. Schnegg, M. Peguiron, and B. V. LeQuang, 1981, An analytic one-dimensional magnetotelluric inversion scheme: Geophysical Journal of the Royal Astronomical Society, **67**, 257–278.

Garcia, X., and A. G. Jones, 2002, Atmospheric sources for audio-magnetotelluric (AMT) sounding: Geophysics, **67**, 448–458.

Goldstein, M. A., and D. W. Strangway, 1975, Audio-frequency magnetotellurics with a grounded electric dipole source: Geophysics, **40**, 669–683.

Guerin, R., and Y. Benderitter, 1995, Shallow karst exploration using MT-VLF and DC resistivity methods: Geophysical Prospecting, **43**, 635–653.

Habberjam, G. M., 1972, The effects of anisotropy on square array resistivity measurements: Geophysical Prospecting, **20**, 249–266.

Li, X., and L. B. Pedersen, 1992, Controlled-source tensor magnetotelluric responses of a layered earth with azimuthal anisotropy: Geophysical Journal International, **111**, 91–103.

Linde, N., and L. B. Pedersen, 2004, Evidence of electrical anisotropy in limestone formations using the RMT technique: Geophysics, **69**, 909–916.

Matias, M. J. S., 2002, Square array anisotropy measurements and resistivity sounding interpretation: Journal of Applied Geophysics, **49**, 185–194.

McNeill, J. D., 1991, Advances in electromagnetic methods for groundwater studies: Geoexploration, **27**, 65–80.

McNeill, J. D., and V. F. Labson, 1989, Geological mapping using VLF radio fields, *in* M. M. Nabighian, ed., Electromagnetic methods in applied geophysics: SEG, 521–640.

Meju, M. A., S. L. Fontes, M. F. B. Oliveira, J. P. R. Lima, E. U. Ulugergerli, and A. A. Carrasquilla, 1999, Regional aquifer mapping using combined VES-TEM-AMT/EMAP methods in the semiarid eastern margin of Parnaiba basin, Brazil: Geophysics, **64**, 337–356.

Newman, G. A., S. Recher, B. Tezkan, and F. M. Neubauer, 2003, 3D inversion of a scalar radio magnetotelluric field data set: Geophysics, **68**, 791–802.

Parker, R. L., and J. R. Booker, 1996, Optimal one-dimensional inversion and bounding of magnetotelluric apparent resistivity and phase measurements: Physics of the Earth and Planetary Interiors, **98**, 269–282.

Parker, R. L., and K. A. Whaler, 1981, Numerical methods of establishing solutions to the inverse problem of electromagnetic induction: Journal of Geophysical Research, **865**, 9574–9584.

Pedersen, L. B., 1982, The magnetotelluric impedance tensor — Its random and bias errors: Geophysical Prospecting, **30**, 188–210.

Pedersen, L. B., M. Bastani, and L. Dynesius, 2005, Ground water exploration using combined controlled source and radiomagnetotelluric techniques: Geophysics, **70**, G8–G15.

Pedersen, L. B., and B. Oskooi, 2004, Airborne VLF measurements and variations of ground conductivity: A tutorial: Surveys in Geophysics, **25**, 151–181.

Pedersen, L. B., W. Qian, L. Dynesius, and P. Zhang, 1994, An airborne tensor VLF system: From concept to realisation, Geophysical Prospecting, **42**, 863–883.

Pedersen, L. B., and T. M. Rasmussen, 1989, Inversion of magnetotelluric data: A non-linear least-squares approach: Geophysical Prospecting, **37**, 669–695.

Qian, W., and L. B. Pedersen, 1992, Near-surface distortion effects on controlled source magnetotelluric transfer-functions: Geophysical Journal International, **108**, 833–847.

Ritzi, R. W., and R. H. Andolsek, 1992, Relation between anisotropic transmissivity and azimuthal resistivity surveys in shallow fractured carbonate flow systems: Ground Water, **30**, 774–780.

Siripunvaraporn, W., and G. Egbert, 2000, An efficient data-subspace inversion method for 2D magnetotelluric data: Geophysics, **65**, 791–803.

Siripunvaraporn, W., G. Egbert, and M. Uyeshima, 2005, Interpretation of two-dimensional magnetotelluric profile data with three-dimensional inversion: Synthetic examples: Geophysical Journal International, **160**,

804–814.
Siripunvaraporn, W., M. Uyeshima, and G. Egbert, 2004, Three-dimensional inversion for network-magnetotelluric data: Earth, Planets and Space, **56**, 893–902.
Smith, A. J., and P. J. Jenkins, 1998, A survey of natural electromagnetic noise in the frequency range f = 1–10 kHz at Halley Station, Antarctica: 1. Radio atmospherics from lightning: Journal of Atmospheric and Solar-Terrestrial Physics, **60**, 263–277.
Stiefelhagen, W., and I. Müller, 1997, Radio frequency electromagnetics (RF-EM) — Extended VLF applied to hydrogeology: 59th Conference and Technical Exhibition, EAGE, Extended Abstracts, F–46.
Takasugi, S., K. Tanaka, N. Kawakami, and S. Muramatsu, 1992, Effectiveness of spatially dense MT measurements for a study of fine resistivity structure — A case-study at Hohi Sugawara, Kyushu, Japan: Journal of Geomagnetism and Geoelectricity, **44**, 223–242.
Tezkan, B., 1999, A review of environmental applications of quasi-stationary electromagnetic techniques: Survey in Geophysics, **20**, 279–308.
Tezkan, B., M. Goldman, S. Greinwald, A. Hördt, I. Müller, F. M. Neubauer, and G. A. Zacher, 1996, Joint application of radiomagnetotellurics and transient electromagnetics to the investigation of a waste deposit in Cologne (Germany): Journal of Applied Geophysics, **34**, 199–212.
Tezkan, B., A. Hördt, and M. Gobashy, 2000, Two-dimensional radiomagnetotelluric investigation of industrial and domestic waste sites in Germany: Journal of Applied Geophysics, **44**, 237–256.
Thiel, D. V., and I. J. Chant, 1982, Ionospheric induced very low-frequency electric field wavetilt changes: Geophysics, **47**, 60–62.
Turberg, P., I. Müller, and F. Flury, 1994, Hydrogeological investigation of porous environments by radio magnetotelluric-resistivity (RMT-R 12–240 kHz): Journal of Applied Geophysics, **31**, 133–143.
Vallée, M. A., M. Chouteau, and G. J. Palacky, 1992a, Effect of temporal and spatial variations of the primary signal on VLF total-field surveys: Geophysics, **57**, 97–105.
———1992b, Variations of the VLF-EM primary field: Analysis of airborne survey data, New Brunswick, Canada: Geophysics, **57**, 181–186.
Wannamaker, P. E., 1997, Tensor CSAMT survey over the sulphur springs thermal area, Valles Caldera, New Mexico, USA: 2. Implications for CSAMT methodology: Geophysics, **62**, 466–476.
Wu, N., J. R. Booker, and J. T. Smith, 1993, Rapid two-dimensional inversion of COPROD2 data: Journal of Geomagnetism and Geoelectricity, **45**, 1073–1087.
Zhang, P., M. Chouteau, M. Mareschal, R. Kurtz, and C. Hubert, 1995, High-frequency magnetotelluric investigation of crustal strucure in north-central Abitibi, Quebec, Canada: Geophysical Journal International, **120**, 406–418.